Journal of Magnetic Resonance **151,** 328–331 (2001)
doi:10.1006/jmre.2001.2374, available online at http://www.idealibrary.com on IDEAL®

COMMUNICATIONS

Sequential HNCACB and CBCANH Protein NMR Pulse Sequences

Axel Meissner and Ole Winneche Sørensen

Department of Chemistry, Carlsberg Laboratory, Gamle Carlsberg Vej 10, DK-2500 Valby, Denmark

Received February 14, 2001; revised April 24, 2001; published online July 3, 2001

The pulse sequences HNCACB and CBCANH correlating side chain C^{β} resonances with amide resonances in the protein backbone do not distinguish between inter- and intraresidue correlations. The new pulse sequences *sequential* HNCACB and *sequential* CBCANH make this distinction by suppressing coherence transfer between $^{13}C^{\alpha}$ and ^{15}N via the one-bond $J(NC^{\alpha})$ coupling so that only the sequential correlations are observed in the spectrum. The experimental results of applying *sequential* HNCACB in a *clean*-TROSY-adapted implementation to the protein Chymotrypsin Inhibitor 2 at 800 MHz are presented.

Key Words: **TROSY**; *sequential* **HNCACB**; *sequential* **CBCANH**; **sequential assignment.**

The pulse sequences CBCANH (*1*) and HNCACB (*2*) are standard tools in protein NMR for linking the assignment of the backbone resonances to the side chains and also for resolving overlap in the C^{α} spectral region typical for proteins with extensive α helical structure. Which of the two experiments to choose depends on the transverse relaxation time of $^{13}C^{\alpha}$ (*3*). For large perdeuterated proteins, only the HNCACB experiment is relevant and shall be used for comparison for the new *sequential* techniques in this paper.

Both HNCACB and CBCANH involve magnetization transfer between $^{13}C^{\alpha}$ and ^{15}N via $J(NC^{\alpha})$ coupling constants in the protein backbone. However, since the one-bond and two-bond $J(NC^{\alpha})$ are of similar magnitude there is no discrimination between the associated two magnetization transfer pathways. Therefore, the resulting spectra show amide groups being correlated with $^{13}C^{\beta}$ resonances of both their own (intra-) and the preceding (inter-) amino acid residues.

If the backbone resonances have been assigned in advance, the assignment of HNCACB or CBCANH spectra can still be done unambiguously if there is no severe overlap of peaks. Another experiment, CBCA(CO)NH (*4*) or HN(CO)CACB, solves this kind of problem by choosing a different magnetization transfer pathway. Rather than transferring directly between the $^{13}C^{\alpha}$ and ^{15}N spins there is a relay step via ^{13}CO where all but the one-bond J coupling constants are insignificant. The result is that only the sequential correlations are observed or in other words that the number of peaks in the spectra is reduced to half. It is an added benefit that the relayed transfer via ^{13}CO often is more efficient than the direct transfer between $^{13}C^{\alpha}$ and ^{15}N nuclei.

However, given that the spectral simplification offered by CBCA(CO)NH or HN(CO)CACB is attractive, the modern trend of performing NMR experiments at higher and higher fields runs into the problem of efficient transverse relaxation of carbonyl carbons by the chemical shift anisotropy mechanism at the high fields. Hence at some point the sensitivity advantage of the ^{13}CO relay transfer is lost and the direct transfer between $^{13}C^{\alpha}$ and ^{15}N becomes the most sensitive approach (*5*).

That then poses the problem of how to achieve the spectral simplification of CBCA(CO)NH or HN(CO)CACB for direct $^{13}C^{\alpha}$–^{15}N magnetization transfers. The solution is the same trick as was used to realize *sequential* HNCA (*6*) that for large molecules at high fields is more sensitive than the conventional approach of HN(CO)CA for obtaining sequential $^{13}C^{\alpha}$ and ^{15}N correlations.

The trick consists of letting the $^{15}N(i)$ magnetization in, e.g., the HNCACB pulse sequence become antiphase with respect to $^{1}J(NC')$ prior to the transfer to $^{13}C^{\alpha}$. This J(NC') antiphase character is carried over to the $^{13}C^{\alpha}$ magnetization immediately after the transfer from ^{15}N. For the interresidue correlation $(i-1)$ via $^{2}J(NC^{\alpha})$ the antiphase character of the $^{13}C^{\alpha}$ magnetization is with respect to $^{1}J(C^{\alpha}C')$, whereas for the intraresidue correlation *(i)* via $^{1}J(NC^{\alpha})$ it is with respect to $^{2}J(C^{\alpha}C')$. Next, a J evolution period on the order of $1/2(^{1}J(C^{\alpha}C'))^{-1}$ for the C^{α} magnetization will refocus the ^{13}CO antiphase character only for the interresidue correlation $(i-1)$ while the magnetization associated with the intraresidue connectivity (i) will not refocus but in fact acquire further antiphase character with respect to the ^{13}CO one bond away (i). The intraresidue doubly antiphase magnetization will not refocus later in the pulse sequence and hence will not lead to observable magnetization.

The *sequential* HNCACB pulse sequence is outlined in Fig. 1a and contains several well-known pulse sequence building blocks. After an initial INEPT transfer from ^{1}H to ^{15}N the ^{15}N magnetization acquires a doubly antiphase character with respect to couplings to the neighboring ^{13}CO spin and one of the $^{13}C^{\alpha}$ spins. Then follows a transfer by two $\pi/2$ pulses to $^{13}C^{\alpha}$ that for the sequential connectivity refocuses the ^{13}CO antiphase

1090-7807/01 $35.00

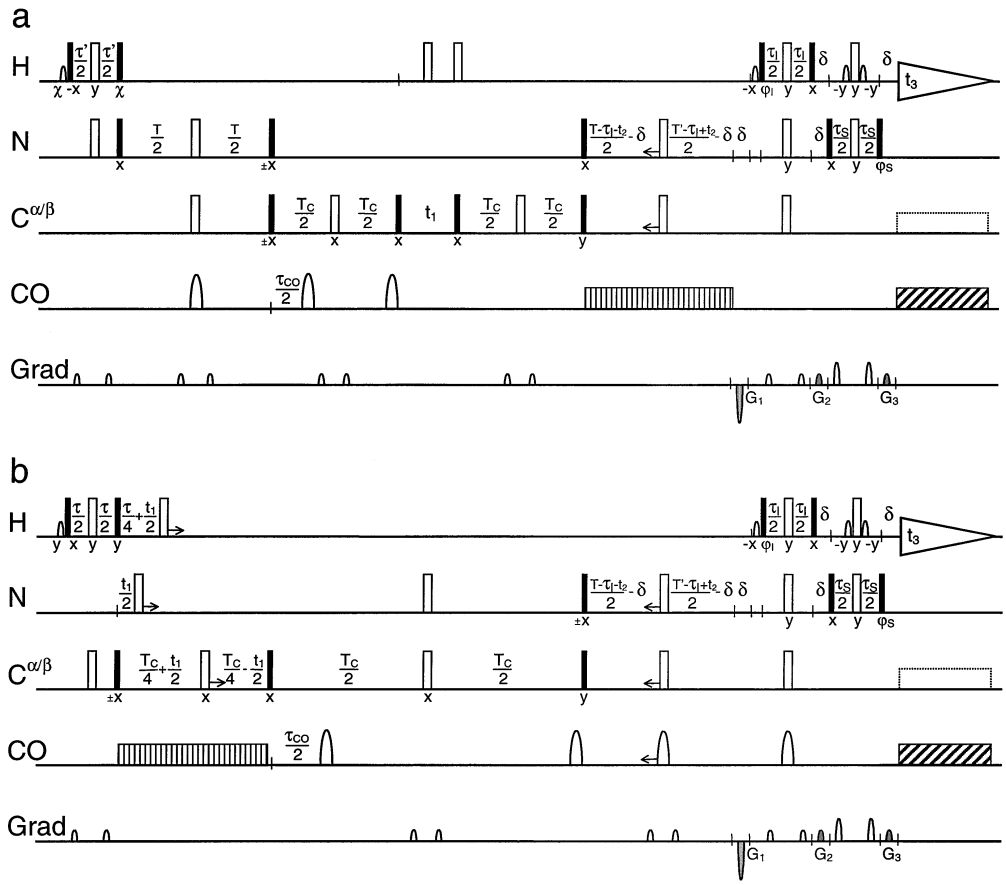

FIG. 1. (a) *Sequential* HNCACB and (b) *sequential* CBCANH pulse sequences employing *clean* TROSY (*7*). Filled and open bars represent $\pi/2$ and π pulses, respectively. Water-selective $\pi/2$ pulses serving to avoid saturation of the water resonance are indicated as open bell shapes. States-TPPI is employed in t_1 and echo-antiecho in $t_2 - t_3$. For Varian instruments, phases $\varphi_I = y$, $\varphi_S = y - \Delta\varphi_S$ and gradient ratios $(G_1 : G_2 : G_3) = (-7 : 3 : 1.987)$ select the echo, whereas the setting $\varphi_I = -y$, $\varphi_S = -y - \Delta\varphi_S$ and $(G_1 : G_2 : G_3) = (-8 : 2 : 3.013)$ selects the antiecho. On Bruker instruments the φ_I and φ_S phases must be inverted. In order to include the native ^{15}N magnetization in sequence (a), χ is $-y$ and y on Varian and Bruker instruments, respectively. The prefix "$\pm$" to pulse phases indicates independent π phase shift two-step cycles with alternating receiver phase. τ_I and τ_S should be adjusted according to *clean* TROSY (*7*) while τ' typically is slightly shorter than $1/2(^1J(NH))^{-1}$ to compensate decay by transverse relaxation. τ in (b) is set to $1/2(^1J(C^\beta H))^{-1}$ or slightly shorter for the INEPT transfer. δ is a gradient delay. T is adjusted for optimum transfer between ^{15}N and $^{13}C^\alpha$ via the $^2J(NC^\alpha)$ coupling constant, with $T' = T -$ the duration of the selective water pulse. τ_{CO} is $1/2(^1J(C'C^\alpha))^{-1}$ to refocus/generate CO antiphase magnetization, and T_C is set slightly shorter than $1/2(^1J(C^\alpha C^\beta))^{-1}$ for magnetization transfer between $^{13}C^\alpha$ and $^{13}C^\beta$. In sequence (a) selective decoupling of CO is applied during the t_2 constant time evolution period, while it is applied during the period with transverse C^β magnetization in (b). Carbon broadband decoupling is employed during acquisition. Pulse programs are available via http://www.crc.dk/nmr/.

character and acquires antiphase character with respect to its neighboring $^{13}C^\beta$. A second $\pi(^{13}CO)$ at the end of the delay compensates the Bloch–Siegert shift introduced by the preceding $\pi(^{13}CO)$ pulse. Next, a $\pi/2$ pulse transfers magnetization from $^{13}C^\alpha$ to $^{13}C^\beta$ that evolve during an evolution period t_1. In the second half of the pulse sequence the same magnetization transfer steps are repeated in opposite order but with coupling to ^{13}CO suppressed throughout. At the end of the sequence, magnetization is transferred from ^{15}N to its attached proton by a *clean* TROSY element (*7*) improving sensitivity and resolution in spectra of large proteins at high fields (*8*). The central $\pi(^1H)$ pulse in the t_1 period serves to suppress $^1J(CH)$, but because it also interchanges TROSY and anti-TROSY resonances, a second $\pi(^1H)$ pulse is necessary at the end of this evolution period. Clearly, this pair of $\pi(^1H)$ pulses should be omitted in experiments on perdeuterated protein samples. For such samples it is advantageous to apply deuterium multipulse decoupling during aliphatic ^{13}C evolution. ^{13}C multipulse decoupling in the pulse sequence is centered in the ^{13}CO spectral region but the first element applies WURST-2 (*9*) to minimize the effect on $^{13}C^\alpha$ while more broadband GARP decoupling (*10*) is applied during $^1H^N$ acquisition because decoupling of $^{13}C^\alpha$ is desirable there.

Figure 2 shows two-dimensional spectra ($t_2 = 0$): at the left a conventional HNCACB spectrum (recorded with the pulse sequence in Fig. 1 without the $\pi(^{13}CO)$ pulses and with appropriate adjustment of pulse phases), in the middle the *sequential* HNCACB spectrum, and at the right a linear combination of the two exhibiting only the intraresidue correlations. The protein investigated was Chymotrypsin Inhibitor 2 (*11, 12*). To appreciate the high degree of discrimination between inter- and

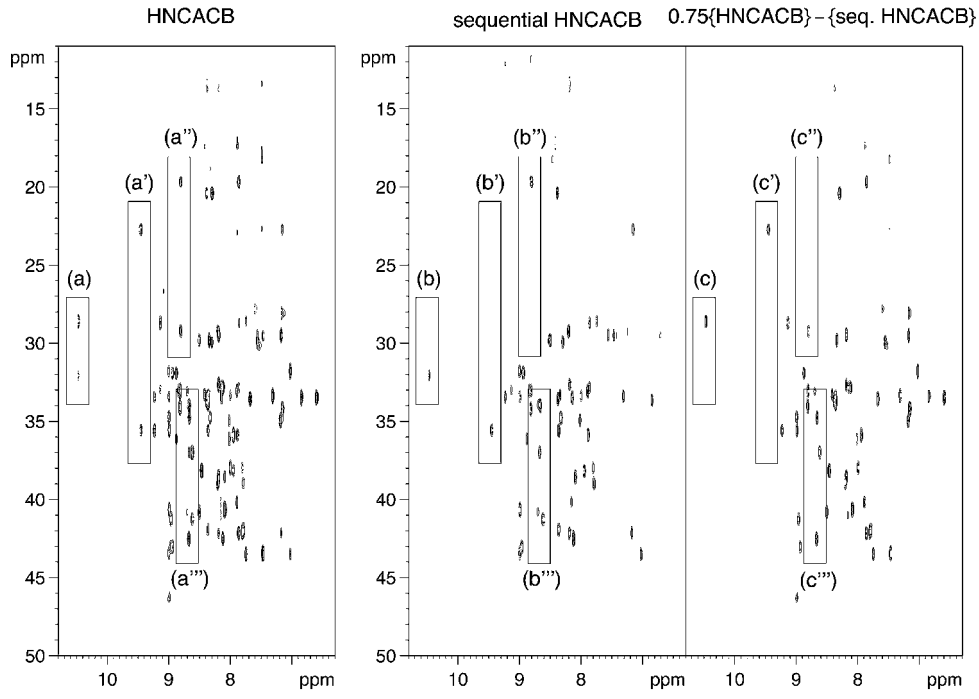

FIG. 2. Comparison of excerpts from the first t_2 interferogram (echo) of the C^β region of HNCACB (left), *sequential* HNCACB (middle), and edited intraresidue HNCACB (right) spectra of ^{15}N,^{13}C-labeled CI2 21-83 (90% H_2O/10%D_2O, 25°C, pH 4.2, 18 mg in 600 μl) recorded on a Varian Unity Inova 800 MHz spectrometer. For *sequential* HNCACB the pulse sequence shown in Fig. 1a was employed. The same sequence was used for HNCACB, where the shaped CO π pulses were omitted, and the phase of the second ^{15}N $\pi/2$ pulse as well as the phase of the first $^{13}C^{\alpha/\beta}$ $\pi/2$ pulse was $\pm y$, Parameters: relaxation delay 1.5 s, $\tau' = \tau_I = \tau_S = 5.43$ ms; $T = 22.00$ ms; $T' = 21.00$ ms; $T_c = 14.27$ ms; $\tau_{CO} = 9.09$ ms; $\delta = 1.10$ ms; t_1(max) = 9.46 ms; 128 scans. Sinc-shaped (*13*) selective $\pi/2$ water pulses (1000.0 μs) and iBurp-shaped (*14*) selective carbon π pulses (931.0 μs) were used. Rectangular $\pi/2$ and π $C^{\alpha/\beta}$ pulses (offset: 36.0 ppm) were calibrated to have a zero excitation profile in the CO region. Adiabatic decoupling of CO during ^{15}N constant time evolution covering 20 ppm was applied using WURST-2 decoupling (*9*); GARP decoupling (*10*) was used during data acquisition. The gradients in the self-compensating pairs had relative amplitudes of 1.0 in the initial INEPT transfer, 0.5 in the T and T_C periods, 1.0 in the first S^3CT element of TROSY transfer, and 6.0 in the final S^3CT/Watergate element. Data matrices of 200 × 2048 points covering 10460 × 12000 Hz were zero-filled to 1024 × 2048 prior to Fourier transformation and the window function was cosine in both dimensions. The intraresidue HNCACB spectrum, showing only HNCACB correlation within the same amino acid, was obtained by linear combination of HNCACB and *sequential* HNCACB spectra in a ratio of 0.75 : −1. F_1 sections along the center of the boxes in the spectra are shown in Fig. 3.

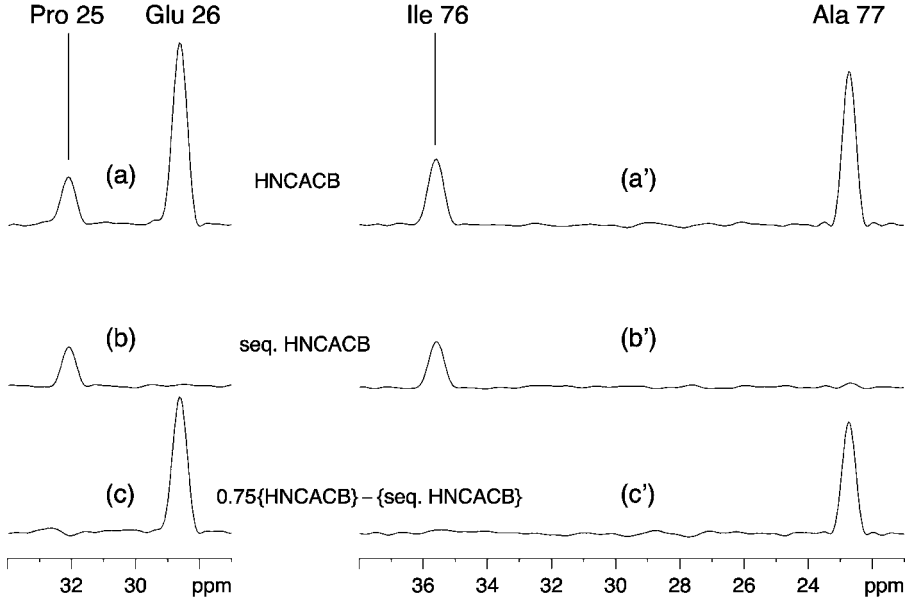

FIG. 3. 1D sections along the center of the boxes as indicated in Fig. 2. (a), (a′), (a″), and (a‴) HNCACB where both sequential ($H_{(i)}$–$C^\beta_{(i-1)}$) and intraresidue ($H_{(i)}$–$C^\beta_{(i)}$) correlations are present. (b), (b′), (b″), and (b‴) *sequential* HNCACB showing only the sequential ($H_{(i)}$–$C^\beta_{(i-1)}$) correlations. (c), (c′), (c″), and (c‴) Linear combination of HNCACB TROSY and *sequential* HNCACB in the ratio of 0.75 : −1 yielding the spectrum containing only intraresidue ($H_{(i)}$–$C^\beta_{(i)}$) correlations.

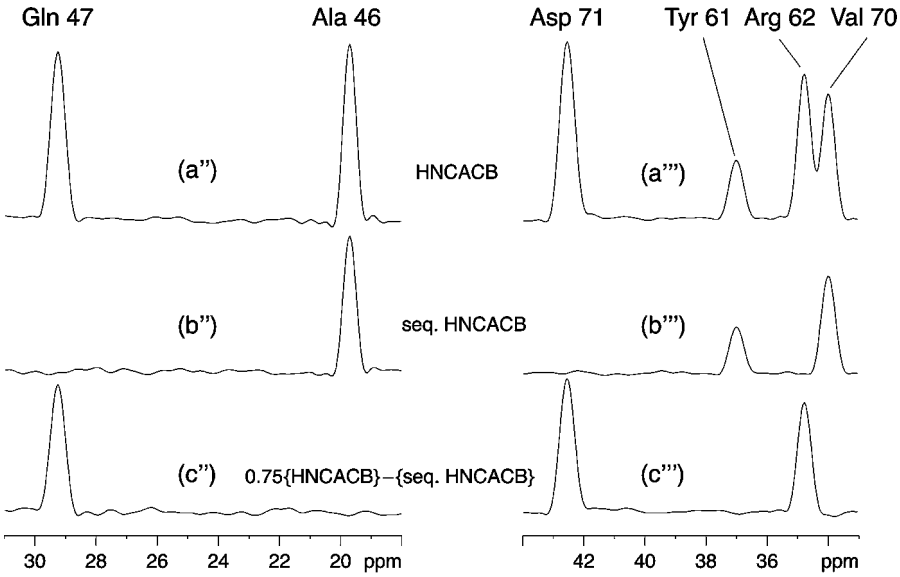

FIG. 3—*Continued*

intraresidue correlations, sections through the regions framed in Fig. 2 are shown in Fig. 3. Recording both the conventional and the *sequential* HNCACB spectra in order to obtain edited intra- and interresidue correlations requires more instrument time, and one may not always want to do that. Should it be desirable, one would record more scans for the *sequential* HNCACB than for the conventional HNCACB in order to compensate for the sequential correlations being weaker.

In conclusion, we have introduced new pulse sequences, *sequential* HNCACB and *sequential* CBCANH, for correlation of $^{15}N(i)$ with interresidue $^{13}C^{\beta}(i-1)$ in side chains of large molecules at high fields. Compared to the conventional techniques the resulting spectra contain only half the peaks.

ACKNOWLEDGMENTS

The spectra presented were recorded on the Varian Unity Inova 800 MHz spectrometer of the Danish Instrument Center for NMR Spectroscopy of Biological Macromolecules at Carlsberg Laboratory. We thank Flemming M. Poulsen, Pia Skovgaard, and Mathilde H. Lerche for the $^{15}N,^{13}C$-labeled Chymotrypsin Inhibitor 2 sample.

REFERENCES

1. S. Grzesiek and A. Bax, *J. Magn. Reson*. **99,** 201–207 (1992).
2. M.Wittekind and L. Mueller, *J. Magn. Reson. B* **101,** 201–205 (1992).
3. M. Sattler, J. Schleucher, and C. Griesinger, *Prog. NMR Spectrosc*. **34,** 93–158 (1999).
4. S. Grzesiek and A. Bax, *J. Am. Chem. Soc*. **114,** 6291–6293 (1992).
5. J. P. Loria, M. Rance, and A. G. Palmer III, *J. Magn. Reson*. **141,** 180–184 (1999).
6. A. Meissner and O. W. Sørensen, *J. Magn. Reson*. **150,** 100–104 (2001).
7. T. Schulte-Herbrüggen and O. W. Sørensen, *J. Magn. Reson*. **144,** 123–128 (2000).
8. K. Pervushin, R. Riek, G. Wider, and K. Wüthrich, *Proc. Natl. Acad. Sci. U.S.A.* **94,** 12,366–12,371 (1997).
9. E. Kupce and G. Wagner, *J. Magn. Reson. Ser. B* **109,** 329–333 (1995).
10. A. J. Shaka, P. B. Barker, and R. Freeman, *J. Magn. Reson*. **64,** 547–552 (1985).
11. P. Osmark, P. Sørensen, and F. M. Poulsen, *Biochemistry* **32,** 11,007–11,014 (1993).
12. J. C. Madsen, O. W. Sørensen, P. Sørensen, and F. M. Poulsen, *J. Biomol. NMR* **3,** 239–244 (1993).
13. A. J. Temps and C. F. Brewer, *J. Magn. Reson*. **56,** 355–372 (1984).
14. H. Geen and R. Freeman, *J. Magn. Reson*. **93,** 93–141 (1991).